IEEE Access
Multidisciplinary | Rapid Review | Open Access Journal

Received March 29, 2019, accepted May 28, 2019, date of publication June 14, 2019, date of current version July 12, 2019.

Digital Object Identifier 10.1109/ACCESS.2019.2923015

Experimental Study on Compatibility of Eco-Friendly Insulating Medium $C_5F_{10}O/CO_2$ Gas Mixture With Copper and Aluminum

YALONG LI[1], YUE ZHANG[1], YI LI[1], FENG TANG[2], QISHEN LV[2], JI ZHANG[1], SONG XIAO[1], JU TANG[1], AND XIAOXING ZHANG[1,3,4]

[1]School of Electrical Engineering and Automation, Wuhan University, Wuhan 430072, China
[2]Shenzhen Power Supply Company, Ltd., Shenzhen 518053, China
[3]State Key Laboratory of Power Transmission Equipment and System Security and New Technology, Chongqing University, Chongqing 400044, China
[4]School of Electrical and Electronic Engineering, Hubei University of Technology, Wuhan 430068, China

Corresponding author: Xiaoxing Zhang (xiaoxing.zhang@outlook.com)

This work was supported in part by the Science and Technology Project of China Southern Power Grid under Grant 090000KK52170114.

ABSTRACT The $C_5F_{10}O$ gas mixture has great application prospects as a potential SF_6 substitute gas. It is necessary to study the compatibility of the $C_5F_{10}O$ gas mixture with copper and aluminum used in the electrical insulation equipment before the engineering application. In this paper, we studied the interaction of $C_5F_{10}O/CO_2$ with copper and aluminum at various temperatures experimentally. The results show that the compatibility of copper with the $C_5F_{10}O/CO_2$ gas mixture is obviously inferior to that of aluminum. Considering the temperature rise effect during normal operation of the equipment, it is found that the interaction between $C_5F_{10}O/CO_2$ gas mixture and copper at 80 °C will lead to slight corrosion on the copper surface. The corrosion degree increased at the higher temperature. SEM shows that massive cubic grains will be formed on the copper surface at 150 °C–250 °C. No corrosion was observed on the aluminum surface at 150 °C∼250 °C, which is related to the protective effect of the oxide layer Al_2O_3 on the aluminum. The relevant results reveal the compatibility of the $C_5F_{10}O/CO_2$ gas mixture with metal materials and provide an important reference for the engineering application of the $C_5F_{10}O$ gas mixture.

INDEX TERMS $C_5F_{10}O/CO_2$, copper, aluminum, compatibility, SF_6 substitute gas.

I. INTRODUCTION

Sulphur hexafluoride (SF_6) has been widely used in gas-insulated equipment since the 1970s for its excellent insulation performance and arc extinguishing performance. At present, the use of SF_6 in the power industry accounts for more than 80% of its annual output. However, the global warming potential (GWP) value of SF_6 is 23,500 times than that of CO_2, and its atmospheric life is as long as 3,200 years [1]–[5], so its emissions will have a long-term impact on the atmospheric environment. The Paris Agreement adopted in 2015 clearly stated that the global mean temperature increase should be controlled within 2°C by the end of this century. Therefore, it is urgent to find environmental friendly alternative gas of SF_6 as an insulating medium for electrical equipment [6].

$C_5F_{10}O$ is one of the hotspots of current researches in replacing SF_6 as a gas insulating medium [7]–[9]. Its dielectric strength is twice that of SF_6, and the GWP value is less than 1. However, its liquefaction temperature of $C_5F_{10}O$ at normal pressure is 26.9 °C, so it is difficult to use as a separate insulating medium, and must be mixed with buffer gas (such as Air, N_2, CO_2) to meet the liquefaction temperature requirements in the equipment [10]–[12].

At present, researches on $C_5F_{10}O$ gas mixtures has achieved many achievements. ABB™ tested the insulation properties and breaking properties of $C_5F_{10}O$ [7], [13]. They found that the insulation performance of $C_5F_{10}O/CO_2/O_2$ gas mixture is only slightly lower than SF_6, and the breaking performance is 30% lower than SF_6. Tatarinov et al. studied the decomposition products of $C_5F_{10}O$ gas mixture

The associate editor coordinating the review of this manuscript and approving it for publication was Bora Onat.

(mixed with N_2 or dry air) based on the principle of Dielectric Barrier Discharge (DBD). Several by-products such as C_4F_{10}, C_6F_{14}, C_3F_6, C_5F_{12} were produced. And it is pointed out that the addition of dry air accelerates the decomposition of $C_5F_{10}O$ [14], [15]. Mingzhe Rong and Xiaohua Wang of Xi'an Jiaotong University studied the saturated vapor pressure characteristics and breakdown characteristics of $C_5F_{10}O/CO_2$ gas mixture under non-uniform electric field [16]. Xingwen Li et al. studied and found that with the increase of $C_5F_{10}O$ concentration in $C_5F_{10}O/CO_2$ gas mixture, the thermophysical properties of $C_5F_{10}O/CO_2$ gas mixture are much close to SF_6 [17].

At present, researches on $C_5F_{10}O$ gas mixture mainly focus on its insulation performance, but there are few reports on the compatibility between $C_5F_{10}O$ gas mixture and metal materials used in electrical equipment. A suitable gas insulating medium should be compatible with the material inside the equipment, ie the gas insulating medium will not react with the material under long-term contact conditions. Due to the large use of copper, aluminum and other metal materials in low-voltage equipment such as gas-insulated switchgear (GIS), and the current-carrying generatrix and switch contacts will have a certain temperature rise due to the thermal effect of current under normal operating conditions [18]. During the operation of the equipment, partial overheating may occur inside equipment such as GIS due to factors such as poor contact of the contacts [19]. Therefore, it is necessary to study the compatibility of $C_5F_{10}O$ gas mixtures with metal materials under temperature rise and overheating fault conditions.

In this paper, a set of test platform for studying the compatibility of $C_5F_{10}O$ gas mixture with metal materials was designed. The compatibility of $C_5F_{10}O/CO_2$ gas mixture (5% $C_5F_{10}O$, 95% CO_2) with copper and aluminum at different temperatures was investigated. The temperature-rise in the normal operation of GIS is mainly due to the heat generated by the thermal effect of the wire resistance when the working current flows through the current-carrying bus. The maximum operating temperature of electrical equipment is 40 °C, and the upper limit of temperature-rise is 75 K according to IEC 61869-1-2007. The experimental temperature setting in this paper was mainly based on relevant standards and related references [20] in the power industry. The topography of metal surface and the composition of mixed gas under different conditions were analyzed based on Gas Chromatography-Mass Spectrometry (GC-MS), Scanning Electron Microscope (SEM) and X-ray photoelectron spectroscopy (XPS). The interaction between gas mixture and copper and aluminum was analyzed. Relevant results not only reveal the compatibility of $C_5F_{10}O/CO_2$ gas mixture with metal materials, but also provide an important reference for the application of $C_5F_{10}O/CO_2$ gas mixture.

II. METHOD

The schematic diagram of the test platform used in this paper is shown in Figure 1. It mainly includes reaction vessel,

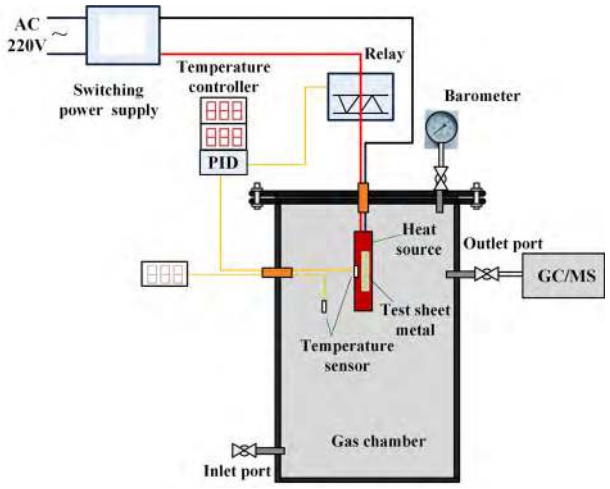

FIGURE 1. Experiment platform.

heat source, temperature sensor, thermostat, GC-MS, SEM, XPS, etc. The reaction vessel was cylindrical with an inner diameter of 126 mm, an outer diameter of 134 mm, a height of 130 mm and a volume of about 1.2 L. The vessel is made of stainless steel. Since the heat source is not in direct contact with the vessel, the temperature of the inner wall of the reactor is low, which avoids the experimental errors caused by the reaction of the inner wall of the reactor. The heat source is placed in the center of the reactor, and the temperature sensor installed on the heat source is connected to the controller for measuring and monitoring the temperature of the heat source to control the test process. A temperature sensor installed in the non-heating zone of the vessel is used to monitor the gas temperature inside the reactor. And barometer is used to monitor the gas pressure inside the reactor.

In the presence of metals, certain chemical reactions may lead to decomposition of $C_5F_{10}O$. These reaction products can be detected and analyzed by GC-MS (GCMS-QP2010 Ultra manufactured by SHIMADZU). SEM was used to characterize the change of the surface morphology of the sample. SEM was selected from the Zeiss SIGMA Field Emission Scanning Electron Microscope (FESEM) manufactured by Carl Zeiss. XPS uses the ESCALAB250Xi electron spectrometer manufactured by Thermo Fisher Scientific of the United States to analyze the changes in the surface element content of the sample.

To facilitate the characterization of the samples after the test, the copper and aluminum samples used in the test were uniformly cut into $0.2\times5\times100$ mm thin slices. After cutting, use ethanol solution to clean the stains on the sample surface, then the residual ethanol on the surface was washed by distilled water, and the sample is placed in a dry box and dried at 35°C for 1 hour. Before the test, the pre-prepared sample was fixed on the heat source, and then the vessel is vacuum-washed three times with CO_2 gas to eliminate interference from other gaseous impurities. After the completion of the scrubbing, the vessel was evacuated to a vacuum by a vacuum pump. First, the vessel was filled with 15 kPa of

FIGURE 2. Photograph of copper samples (the long strip of metal in the figure are test samples). (a) Control group. (b) 150 °C. (c) 200 °C. (d) 250 °C.

FIGURE 3. Photograph of aluminum samples (the long strip of metal in the figure are test samples). (a) Control group. (b) 150 °C. (c) 200 °C. (d) 250 °C.

$C_5F_{10}O$, and then charged with CO_2 to a total gas pressure of 0.3 MPa (absolute pressure). After the aeration was completed, the reactor is allowed to stand for 24 h to ensure gases are evenly mixed [21]. Test temperature are set to 150°C, 200°C and 250°C by temperature controller. The heating time of each test is 8h and the radiating time is 1h.

III. RESULTS AND DISCUSSION

A. MORPHOLOGY CHARACTERIZATION

After the test, gas samples were collected from the reactor and tested by GC-MS. The residual gas was evacuated using the vacuum pump before the vessel is opened. The color contrast of copper slices at different test temperatures is shown in Figure 2.

It can be seen from Figure 2 that there is a significant difference in the color of the copper surface at different test temperatures. The copper surface emits a pungent odor, indicating that the copper is significantly corroded in the $C_5F_{10}O/CO_2$ atmosphere. The surface color of unreacted copper is purple red with bright and uniform distribution. The color of copper exposed in $C_5F_{10}O/CO_2$ atmosphere at 150°C for 8h becomes light brown, and the surface color distribution is slightly uneven, indicating that the copper surface has been corroded. When the test temperature reaches to 200°C, the color of the copper becomes dark brown, and the color distribution is uniform, indicating that the corrosion is already serious. As the temperature rise to 250°C, the color of the copper turn to brownish red, and the color distribution is even, indicating that the corrosion is more serious. In summary, as the test temperature increases, the surface color of the copper in the $C_5F_{10}O/CO_2$ atmosphere gradually changes from purple to brown. The law of color change can initially reflect the severity of corrosion of copper slices by $C_5F_{10}O/CO_2$ gas mixture. This also indicates that the copper electrode has poor compatibility with $C_5F_{10}O/CO_2$ gas mixture under temperature rise and local overheating.

The surface color comparison of the aluminum sample is shown in Figure 3. The aluminum surface did not change significantly before and after the test. It is concluded that the change in the color of the Aluminum surface cannot be used to determine whether the Aluminum and $C_5F_{10}O/CO_2$ gas mixture are compatible.

FIGURE 4. Photograph of copper samples (the long strip of metal in the figure are test samples). (a) 80 °C. (b) 100 °C.

In order to further investigate the initial temperature of copper corrosion of $C_5F_{10}O/CO_2$ gas mixture, another two tests were carried out and test temperatures was set to 100 °C and 80 °C. The test results are shown in Figure 4.

As can be seen from the above figure, the surface of the copper is slightly corroded at 100 °C, and only some areas have color changes. There is no significant color change before and after the test at 80°C. Thus, it is preliminarily determined that the initial temperature of copper corrosion by the $C_5F_{10}O/CO_2$ gas mixture is around 100 °C.

In summary, when the temperature changes from 80 °C to 250°C, the corrosion of copper surface begins to appear and gradually become serious with the increase of temperature. The surface color gradually turns brown and then turns brownish red. No obvious surface morphology changes were observed on the aluminum surface after interacted with $C_5F_{10}O/CO_2$ gas mixture in the range of test temperature 150°C-250°C.

B. GASEOUS BY-PRODUCTS DETECTED BY GC-MS

Since the decomposition component of the $C_5F_{10}O/CO_2$ gas mixture after contact with the sample is unknown, the GC-MS SCAN mode was used to scan all components for chromatography and mass spectrometry. The relative molecular mass of the buffer gas CO_2 used in this test is 44, which is lower than the relative molecular mass of the simplest

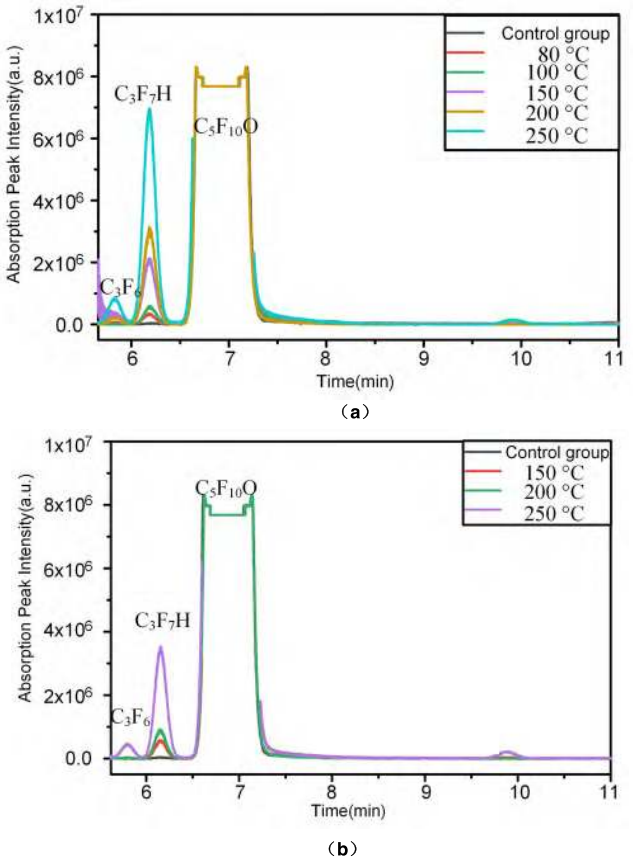

FIGURE 5. Trend of GC-MS pattern of $C_5F_{10}O/CO_2$ gas mixture at different experimental temperatures. (a) Trend of GC-MS pattern of $C_5F_{10}O/CO_2$ gas mixture in contact with copper surface at different temperatures. (b) Trend of GC-MS pattern of $C_5F_{10}O/CO_2$ gas mixture in contact with aluminum surface at different temperatures.

fluorocarbon (CF_4 relative molecular mass 90) and the upper limit of detection of MS detector is several thousand parts per million(ppm) (volume fraction <1%). It can be seen from Figure 5 that the $C_5F_{10}O$ gas concentration in this experiment has far exceeded the detection limit of the detector. In order to protect the detector, avoid its supersaturation and avoid the interference of N_2, H_2O and CO_2 in the air, only substances with $45 \leqslant m/z \leqslant 350$ are detected, and small molecular substances with a mass-to-charge ratio (m/z) of less than 44 are discarded. The mass-to-charge ratio refers to the molecular weight of characteristic ions generated by the collision of electrons after gas molecules enter the mass spectrometer. The CO_2 chromatographic separation time was 5.15-5.57 min. And generally the molecule can pass through the detector within 10 minutes. Figure 5(a) plots the GC-MS chromatogram of the $C_5F_{10}O/CO_2$ gas mixture with a copper surface exposed to different test temperatures for 5.57-11 min.

It can be seen from Fig. 5(a) that the mass spectrum corresponding to the peak of 5.68-5.93 min shows the peak-to-peak mass-to-charge ratio ($m/z = 131$), the molecular ion $m/z = 150$, and the matching molecule of NIST14 database similarity is C_3F_6. The mass spectrum corresponding to the peak of 5.98-6.34min shows the peak-to-peak mass-to-charge ratio ($m/z = 69$), and the matching molecule of NIST14 database similarity is C_3F_7H.

It can be seen from the figure that the $C_5F_{10}O/CO_2$ gas mixture reacts with the copper surface when the test temperature is increased, so that a small part of the $C_5F_{10}O$ molecule is broken to form decomposition products such as C_3F_6 and C_3F_7H. And with the increase of temperature, the concentration of gas decomposition by-products also gradually increased, indicating that the decomposition amount of $C_5F_{10}O$ gradually increased.

Figure 5b is the GC-MS chromatogram of the $C_5F_{10}O/CO_2$ gas mixture exposed to the aluminum surface at 5.57-11 min at different test temperatures. Both Figure 5(a) and Figure 5(b) show a regular increase in the concentration of gaseous by-products with increasing temperature, and the same gaseous by-products appear. However, at the same test temperature, Figure 5b is about 50% smaller than the peak area of Figure 5a, and according to the principle of the area internal standard method for gas quantitative analysis, the concentration of the decomposition product in Figure 5a is about twice that of Figure 5b. This indicates that the compatibility of aluminum with $C_5F_{10}O/CO_2$ gas mixture is much better than that of copper under the same conditions. This is also consistent with the experimental phenomenon.

C. SURFACE TOPOGRAPHY

In order to analyze the micro-morphological changes of copper and aluminum surfaces, the copper samples and aluminum samples before and after the test were characterized by Field Emission Scanning Electron Microscope (FESEM). The surface structure is shown in Figure 6 and Figure 7.

It can be seen from Figure 6 that the copper surface of the control group have fine streaks on its surface when the magnification is 2000X under the microscope due to the manufacturing process limitation, and no corrosion point exists in the entire field of view. When the test temperature is 80°C, some small corrosion spots begin to appear on the surface when magnification is 50000X. The distribution of corrosion points is uneven, and the structural integrity of the surface was destroyed, indicating that copper begins to be corroded in $C_5F_{10}O/CO_2$ atmosphere at this temperature. When the temperature rises to 100°C, the corrosion point of the copper surface gradually enlarges, and the corrosion spots with uneven size and distribution can be seen on the whole sample surface. The areas of these corrosion points are bright under the microscope (at the red mark in the figure). It can be observed that the corrosion gradually covers the entire copper surface when the temperature rises from 150°C to 250°C. Regular cubic block crystal grains appears after the copper surface is corroded and the massive crystal grains gradually become larger as the temperature increases. Significant changes in copper surface have been observed at 2000X magnification at temperatures of 200°C and 250°C. The massive grains produced by the corrosion make the

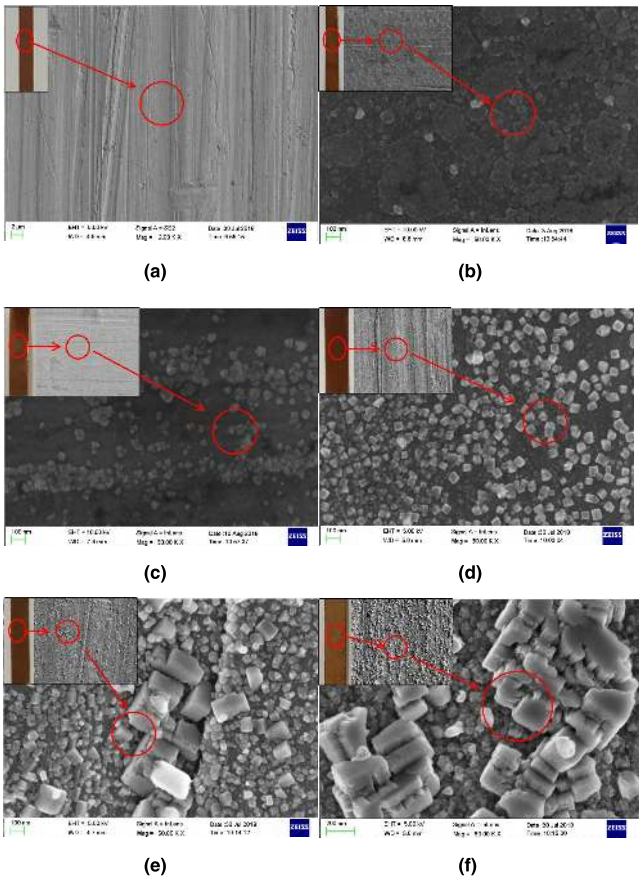

FIGURE 6. SEM photograph of copper samples. (a) SEM photograph of pre-tested copper sample. (b) SEM photograph of copper sample with reaction temperature of 80 °C. (c) SEM photograph of copper sample with reaction temperature of 100 °C. (d) SEM photograph of copper sample with reaction temperature of 150 °C. (e) SEM photograph of copper sample with reaction temperature of 200 °C. (f) SEM photograph of copper sample with reaction temperature of 250 °C.

copper surface begin to roughen, and the corrosion is most severe at 250°C. The bulk grains have covered the surface grooves caused by the manufacturing process.

From the electron microscope results above, it can be seen that copper has poor compatibility with $C_5F_{10}O/CO_2$ gas mixture and it will react strongly with $C_5F_{10}O/CO_2$ gas mixture at high temperature, which will cause obvious changes in surface morphology. Significant corrosion points have occurred at 100°C, which is even lower than the highest temperature limit of GIS equipment (105°C) [22]. Therefore, when the $C_5F_{10}O/CO_2$ gas mixture is used as the insulating medium, the surface of the copper used in the electrical equipment should be treated with anti-corrosion treatment. It can prevent the copper material inside the equipment from corroding when the temperature rises during the operation of the equipment or due to contact action, loose parts, etc., which further deteriorates the operating environment of the electrical equipment. In the long-term consideration, in the equipment using $C_5F_{10}O/CO_2$ gas mixture as the insulating medium, the contact of the current-carrying copper conductor with $C_5F_{10}O$ for a long time will cause electrical equipment

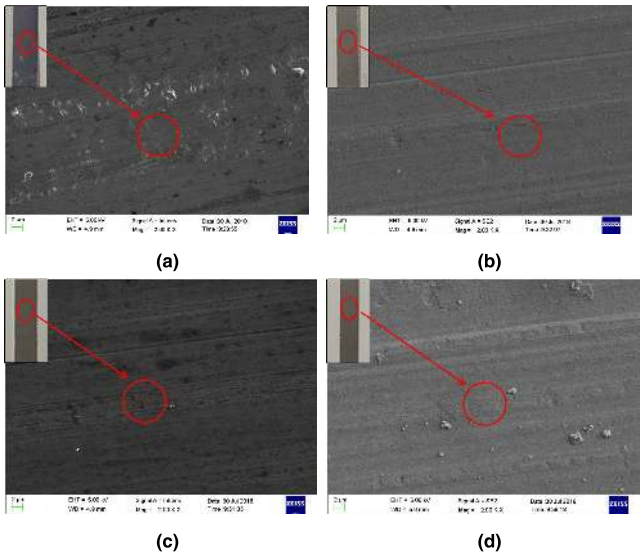

FIGURE 7. SEM photograph of aluminum samples. (a) SEM photograph of pre-tested aluminum sample. (b) SEM photograph of aluminum sample with reaction temperature of 150 °C. (c) SEM photograph of aluminum sample with reaction temperature of 200 °C. (d) SEM photograph of aluminum sample with reaction temperature of 250 °C.

insulation failure and shorten the service life of electrical equipment.

It can be seen from Figure 7 that the aluminum surface is relatively flat, and no change in morphology is observed under the electron microscope before and after the reaction. The aluminum surface after the surface cleaning treatment before the test is shown in Figure 7a. The surface is relatively flat. And the surface morphology of test groups is consistent with the control group at temperatures of 150 °C, 200 °C and 250 °C. No corrosion points were found.

Although the chemical properties of aluminum are more active than copper, the aluminum surface does not undergo corrosion similar to copper at elevated temperatures. This may due to that aluminum has a dense layer of Al_2O_3 oxide formed soon after the surface is exposed to air before the test, which prevent aluminum from corrosion.

D. XPS RESULTS

XPS spectra of copper and aluminum samples were scanned and the Gaussian fitting of XPS spectra was performed in order to analyze the changes of surface element composition. The energy spectra of Cu 2p, F 1s, O 1s and C 1s on the copper surface are shown in Figure 8.

Figure 8a shows the energy spectrum of Cu 2p orbital. It can be seen that the energy spectrum of copper element in 2p electron orbital is mainly four peaks with electron binding energy of 932.7 eV, 934.6 eV, 952.5 eV and 952.7 eV, representing Cu_2O $2p_{3/2}$, CuO $2p_{3/2}$, Cu_2O $2p_{1/2}$, and CuO $2p_{1/2}$. It can be seen from the energy spectrum of copper that the copper element on the surface of the copper sample mainly comes from copper elemental and copper oxide (CuO). As the temperature increases, the relative content of copper is increasing. Combining the energy spectrum curve

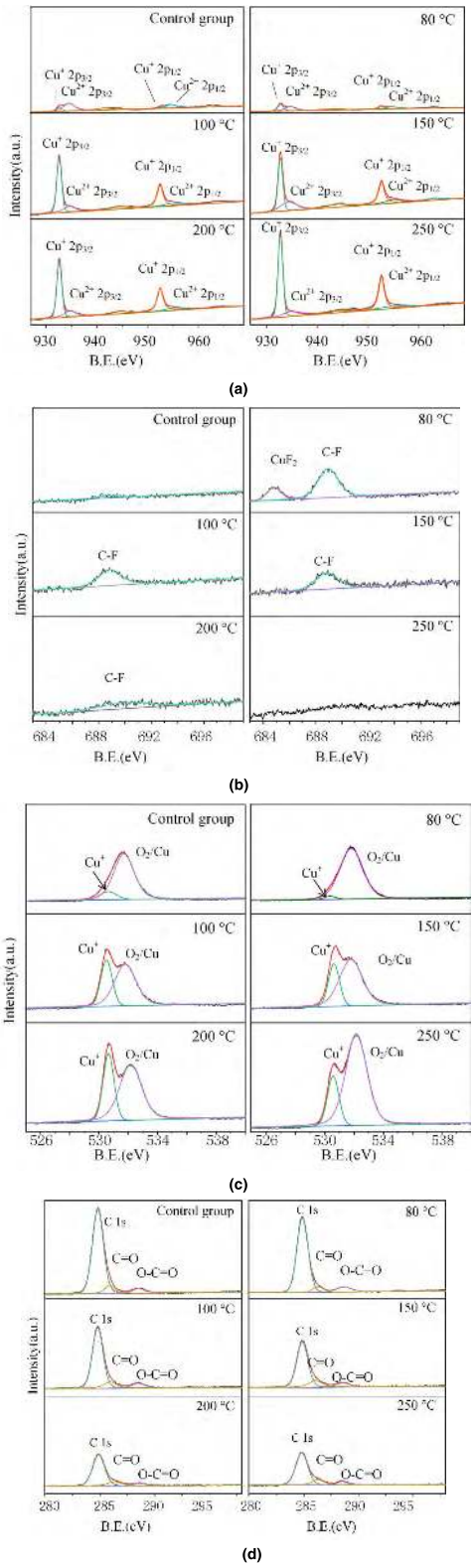

FIGURE 8. Copper surface element XPS energy spectrum. (a) Cu 2p. (b) F 1s. (c) O 1s. (d) C 1s.

of the oxygen element in Figure 8c with the change of the topography of the through surface in Figure 6, the increase in the elemental content of copper is due to the uneven surface of the copper sample, which causes the relative content of Cu, C and O_2 originally covered on the surface to decrease.

Figure 8b shows the energy spectrum of the F 1s orbital, The F1s electron orbitals on the copper surface was detected C-F and CuF_2 at electronic binding energies of 688.8 eV, 684.7 eV at different temperature test groups. No fluorine was detected on the copper surface of the control group, indicating that there is no fluorine residue on the sample surface. When the test temperature is 80°C, C-F and CuF_2 were detected on the sample surface. When the temperature is further increased, there is no CuF_2 on the sample surface, and the relative content of C-F is gradually decreased. When the temperature is increased to 250°C, no fluorine element is detected on the sample surface. It can be seen from the above test results that $C_5F_{10}O$ could react with copper to form CuF_2 firstly, which will adhere to the copper surface. The detection of C-F may be due to the adhesion of part of $C_5F_{10}O$ to the copper surface. The XPS spectrum shows that the fluorine-containing compound will adhere to the surface of the copper material only when the test temperature is below 250 °C. Once the temperature is too high, the adhesion of the fluorine-containing compound will be inhibited.

Figure 8c shows the energy spectrum of the O1s electron orbital. The presence of O_2/Cu (oxygen on copper, O_2^-, O^{2-} or O^-) and Cu_2O were detected at electron binding energies of 530.8 eV and 531.8 eV. Oxygen on copper may be due to exposure of copper samples to air prior to testing, and oxygen in the air is adsorbed on the copper surface.

Figure 8d shows the energy spectrum of the C1s electron orbit. C, C = O and C-O = O were detected at 284.7 eV, 286.4 eV and 288.6 eV. As the test temperature increases, the relative content of carbon element gradually decreases.

XPS results showed that the surface of the copper sample contained Cu_2O and CuO. The crystal color of Cu_2O is red, while CuO is black. The relative change of Cu_2O and CuO content will affect the color change of copper surface. According to the simulation results of the reference [23], the carbonyl group (C = O) in the $C_5F_{10}O$ molecule has chemically active, and chemical reaction occurs when it contacts the copper at the gas-solid interface. The changes in the contents of Cu_2O, CuO and CuF_2 in the XPS test results also indicate that copper participates in the chemical reaction process.

Figure 9 shows the XPS spectrum of the surface of an aluminum sample. The energy spectrum of the 2p electron orbital of Al element detected Al_2O_3 2p and Al_2O_3 $2p_{3/2}$ at electron binding energies of 74.30 eV and 71.40 eV. This also indicates that the aluminum on the surface of the aluminum sample mainly exists in the state of Al_2O_3. The content of fluorine on the surface of aluminum sample showed a different tendency from that of copper sample. During increase of the test temperature, the fluorine element adhered to the surface of the aluminum sample, and the higher the temperature, the higher the fluorine content, C-F is the only bond of fluorine on the aluminum surface. This also reflects the stability of aluminum materials, Because of the protection

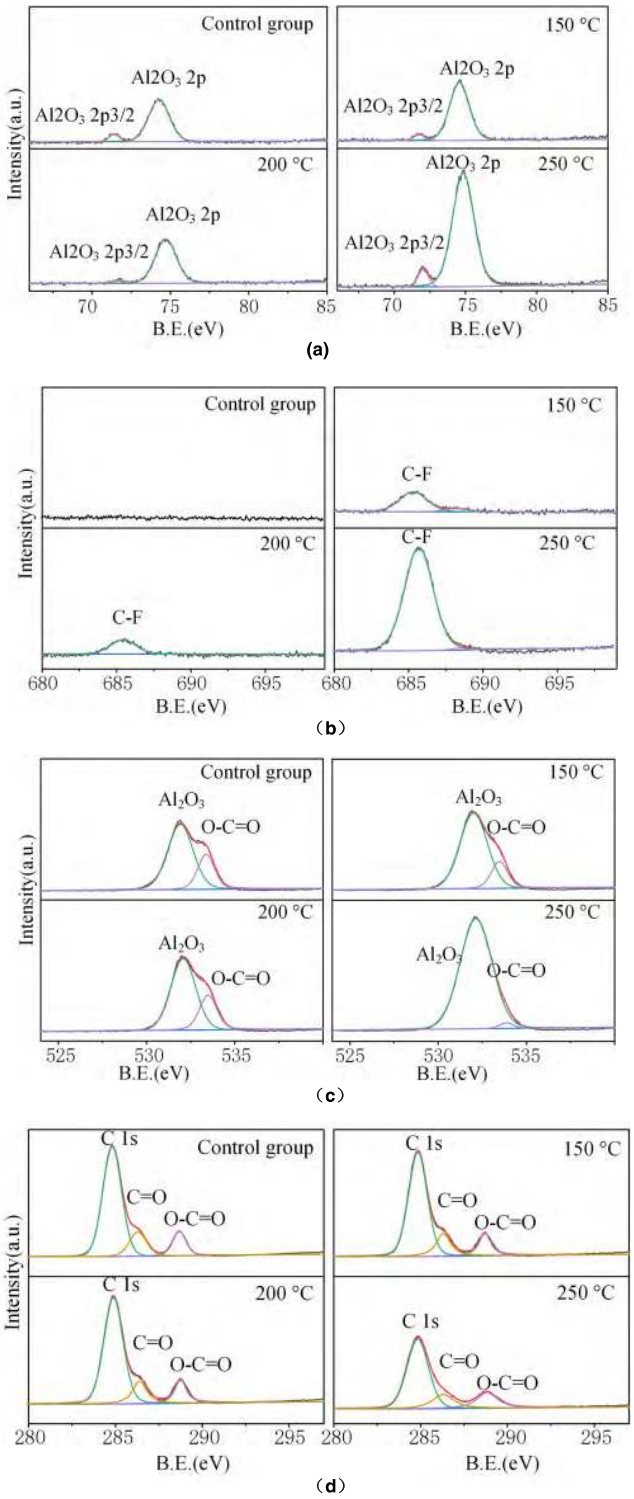

FIGURE 9. **Aluminum surface element XPS energy spectrum. (a) Al 2p. (b) F 1s. (c) O 1s. (d) C 1s.**

of the surface oxide layer Al_2O_3, aluminum does not react similarly to the copper material to form metal fluoride. And the content of oxygen and carbon shows a similar pattern to the surface of copper samples.

It can be seen from the XPS test results that aluminum exhibits higher stability than copper, which is also consistent with the SEM results. Copper reacts with $C_5F_{10}O/CO_2$ mixed gas to form metal fluoride (CuF_2, etc.) during the test. The oxide layer (Al_2O_3) on the surface of the aluminum sample prevents the aluminum from reacting with the $C_5F_{10}O/CO_2$ mixed gas. In summary, the compatibility of aluminum with $C_5F_{10}O/CO_2$ mixed gas is better than that of copper and $C_5F_{10}O/CO_2$ mixed gas at 150-250°C.

IV. CONCLUSION

The compatibility of the gas and metal materials before the application of the SF_6 replacement gas is of great significance to the operational stability and service life of the equipment. In this paper, the compatibility of environmental friendly insulating medium $C_5F_{10}O/CO_2$ gas mixture and metallic materials copper and aluminum in GIS equipment was tested,. The composition of gas mixture and metal samples were analyzed by GC-MS, SEM and XPS. Relevant conclusions can be obtained as follows:

(1) When the test temperature is changed from 80-250 °C, the corrosion of the copper sample in $C_5F_{10}O/CO_2$ atmosphere gradually deepens, a pungent odor scatters from the surface of the sample and the surface color appears to change from purple to brown to brown to red. In contrast, the surface color of aluminum materials has not changed at 150-250°C.

(2) GS-MS, SEM and XPS characterization results show that copper reacts with $C_5F_{10}O/CO_2$ gas mixture during the test. The corrosion point begins to appear on the copper surface at 80°C. As the test temperature increases, the corrosion gradually deepens and the surface forms a block-shaped cubic crystal that gradually becomes larger.

(3) The compatibility of aluminum with $C_5F_{10}O/CO_2$ mixed gas is better than that of copper. It is recommended that the surface of the copper material should do anti-corrosion treatment to avoid the reaction between copper and $C_5F_{10}O/CO_2$ gas mixture for engineering application.

REFERENCES

[1] G. Myhre, *Anthropogenic and Natural Radiative Forcing. Climate Change 2013: The Physical Science Basis. Contribution of Working Group I to the Fifth Assessment Report of the Intergovernmental Panel on Climate Change*. Cambridge, U.K.: Cambridge Univ. Press, 2013.

[2] Y. Kieffel, "Characteristics of G_3- an alternative to SF_6," in *Proc. IEEE Int. Conf. Dielectr. (ICD)*, Jul. 2016, pp. 880–884.

[3] S. K. Allen, G. K. Plattner, A. Nauels, Y. Xia, and T. F. Stocker, "Climate change 2013: The physical science basis. An overview of the working group 1 contribution to the fifth assessment report of the intergovernmental panel on climate change (IPCC)," *Comput. Geometr*, vol. 18, no. 2, pp. 95–123, 2007.

[4] J. Tang, F. Liu, X. Zhang, Q. Meng, and J. Zhou, "Partial discharge recognition through an analysis of SF_6 decomposition products part 1: Decomposition characteristics of SF_6 under four different partial discharges," *IEEE Trans. Dielectr. Electr. Insul.*, vol. 19, no. 1, pp. 29–36, Feb. 2012.

[5] X. Zhang, H. Xiao, J. Tang, Z. Cui, and Y. Zhang, "Recent advances in decomposition of the most potent greenhouse gas SF_6," *Crit. Rev. Environ. Sci. Technol.*, vol. 47, no. 18, pp. 1763–1782, Sep. 2017.

[6] A. Romero, L. Rácz, A. Mátrai, T. Bokor, and R. Cselkó, "A review of sulfur-hexafluoride reduction by dielectric coatings and alternative gases," in *Proc. 6th Int. Youth Conf. Energy (IYCE)*, Jun. 2017, pp. 1–5.

[7] J. D. Mantilla, N. Gariboldi, S. Grob, and M. Claessens, "Investigation of the insulation performance of a new gas mixture with extremely low GWP," in *Proc. IEEE Elect. Insul. Conf. (EIC)*, Jun. 2014, pp. 469–473.
[8] X. Zhang, Y. Li, S. Xiao, J. Tang, S. Tian, and Z. Deng, "Decomposition mechanism of C5F10O: An environmentally friendly insulation medium," *Environ. Sci. Technol.*, vol. 51, no. 17, pp. 10127–10136, Aug. 2017.
[9] J. Mantilla, M. Claessens, and M. Kriegel, "Environmentally friendly perfluoroketones-based mixture as switching medium in high voltage circuit breakers," CIGRE Paris, France, Tech. Rep. A3-113, 2016.
[10] Y. Li, X. Zhang, S. Xiao, Q. Chen, and D. Wang, "Decomposition characteristics of $C_5F_{10}O$/air mixture as substitutes for SF_6 to reduce global warming," *J. Fluorine Chem.*, vol. 208, pp. 65–72, Apr. 2018.
[11] Y. Wu, C. Wang, H. Sun, M. Rong, A. B. Murphy, T. Li, J. Zhong, Z. Chen, F. Yang, and C. Niu, "Evaluation of SF_6-alternative gas C_5-PFK based on arc extinguishing performance and electric strength," *J. Phys. D, Appl. Phys.*, vol. 50, no. 38, 2017, Art. no. 385202.
[12] Y. Kieffel, F. Biquez, P. Ponchon, and T. Irwin, "SF_6alternative development for high voltage Switchgears," in *Proc. IEEE Power Energy Soc. Gen. Meeting*, Jul. 2015, pp. 1–5.
[13] P. C. Stoller, C. B. Doiron, D. Tehlar, P. Simka, and N. Ranjan, "Mixtures of CO_2 and $C_5F_{10}O$ perfluoroketone for high voltage applications," *IEEE Trans. Dielectr. Electr. Insul.*, vol. 24, no. 5, pp. 2712–2721, Oct. 2017.
[14] A. V. Tatarinov, I. V. Bilera, S. V. Avtaeva, V. A. Shakhatov, P. V. Solomakhin, R. Maladen, C. Prévé, and D. Piccoz, "Dielectric barrier discharge processing of trans-CF_3CH=CHF and $CF_3C(O)CF(CF3)_2$, their mixtures with Air, N2, CO2 and analysis of their decomposition products," *Plasma Chem. Plasma Process.*, vol. 35, no. 5, pp. 845–862, Sep. 2015.
[15] A. V. Tatarinov, I. V. Bilera, S. V. Avtaeva, V. A. Shakhatov, P. V. Solomakhin, R. Maladen, C. Prévé, and D. Piccoz, "Comparative study of degradation of trans-1, 3, 3, 3-trifluoropropene, 2, 3, 3, 3-tetrafluoropropene, perfluoro-3-methylbutanone-2, and sulfur hexafluoride in dielectric-barrier discharge," *High Energy Chem.*, vol. 50, no. 1, pp. 64–70, Jan. 2016.
[16] J. Zhong, X. Fu, A. Yang, G. Han, J. Liu, Y. Lu, X. Wang, and M. Rong, "Insulation performance and liquefaction characteristic of $C_5F_{10}O/CO_2$ gas mixture," in *Proc. 4th Int. Conf. Elect. Power Equip. Switching Technol.*, Oct. 2017, pp. 291–294.
[17] X. Li, X. Guo, A. B. Murphy, H. Zhao, J. Wu, and Z. Guo, "Calculation of thermodynamic properties and transport coefficients of $C_5F_{10}O$-CO_2 thermal plasmas," *J. Appl. Phys.*, vol. 122, no. 14, 2017, Art. no. 143302.
[18] J.-H. Yoon, H.-S. Ahn, J. Choi, and I.-S. Oh, "An estimation technology of temperature rise in GIS bus bar using three-dimensional coupled-field multiphysics," in *Proc. Conf. Rec. IEEE Int. Symp. Elect. Insul.*, Jun. 2008, pp. 432–436.
[19] Y. Li, X. Zhang, X. Li, Z. Cui, and H. Xiao, "Detection of ozone and nitric oxide in decomposition products of air-insulated Switchgear using ultraviolet differential optical absorption spectroscopy (UV-DOAS)," *Appl. Spectrosc.*, vol. 72, no. 8, pp. 1244–1251, Aug. 2018.
[20] C. T. Dervos, P. Vassiliou, and J. A. Mergos, "Thermal stability of SF_6 associated with metallic conductors incorporated in gas insulated switchgear power substations," *J. Phys. D, Appl. Phys.*, vol. 40, no. 22, p. 6942, 2007.
[21] M. Hikita, S. Ohtsuka, S. Okabe, and S. Kaneko, "Insulation characteristics of gas mixtures including perfluorocarbon gas," *IEEE Trans. Dielectr. Electr. Insul.*, vol. 15, no. 4, pp. 1015–1022, Aug. 2008.
[22] Y. Yamagata, N. Shimoda, Y. Shimizu, M. Ohno, M. Kobayashi, and K. Sasamori, "Field tests on current carrying performances of 1000 kV GIS," in *Proc. IEEE Transmiss. Distrib. Conf.*, Apr. 1999, pp. 495–500.
[23] Y. Li, X. Zhang, S. Xiao, D. Chen, Q. Chen, and D. Wang, "Theoretical evaluation of the interaction between C_5-PFK molecule and Cu(111)," *J. Fluorine Chem.*, vol. 208, pp. 48–54, Apr. 2018.

YALONG LI was born in Zhumadian, Henan, China, in 1989. He received the bachelor's degree in electrical engineering from Wuhan University, Wuhan, China, where he is currently pursuing the Ph.D. degree with the School of Electrical Engineering and Automation. His research interests include SF_6 abatement technology and alternative gas of SF_6.

YUE ZHANG was born in Fuzhou, Jiangxi, in 1995. He received the bachelor's degree in electrical engineering from the Hubei University of Technology. He is currently pursuing the master's degree with the School of Electrical Engineering and Automation, Wuhan University, China. He is mainly involved in online monitoring of high-voltage equipment insulation.

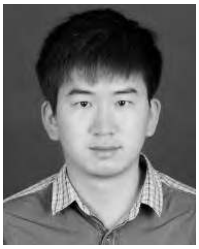

YI LI was born in Shangluo, Shanxi, China, in 1994. He received the bachelor's degree in electrical engineering from Wuhan University, Wuhan, China, where he is currently pursuing the Ph.D. degree with the School of Electrical Engineering and Automation. His research interests include alternative gas of SF_6 and fault diagnosis of high-voltage electrical insulation equipment.

FENG TANG is a Senior Engineer and a Technical Expert, mainly engaged in electrical test work. He is currently with Shenzhen Power Supply Co., Ltd., Shenzhen.

QISHEN LV was born in 1985. He graduated in electrical engineering from Xi'an Jiaotong University, in 2007. He received the master's degree in engineering from Beijing Jiaotong University, in 2014. He is a Senior Engineer with Hulunbeier, Inner Mongolia, China. He is currently with Shenzhen Power Supply Co., Ltd., Shenzhen. He has been engaged in power equipment status testing and operation and maintenance technology for a long time.

JI ZHANG was born in Dongying, Shandong, China, in 1990. He received the bachelor's degree in electrical engineering and automatic chemistry from Shandong Jianzhu University, China. He is currently pursuing the M.A. degree with the School of Electrical Engineering and Automation, Wuhan University. His research interest includes alternative gas of SF_6.

SONG XIAO was born in Zhangjiakou, Hebei, China, in 1988. He received the B.S. and Ph.D. degrees in electrical engineering from Chongqing University, Chongqing, China, and the Ph.D. degree in plasma engineering from the Université de Toulouse, Toulouse, France. He is currently a Postdoctoral Researcher with the School of Electrical Engineering and Automation, Wuhan University. His research interests include partial discharge online monitoring and gas substituting SF_6.

JU TANG was born in Pengxi, Sichuan, China, in 1960. He received the B.Sc. degree from Xi'an Jiaotong University, Xi'an, China, and the M.Sc. and Ph.D. degrees from Chongqing University, Chongqing, China. He is currently a Professor with the School of Electrical Engineering and Automation, Wuhan University, and the Chief Scientist presiding over the National Basic Research Program of China (973 Program) (2009CB724506). At present, he is involved in high-voltage equipment online monitoring, fault diagnosis, signal processing, simulation analysis, and pattern recognition.

XIAOXING ZHANG was born in Qianjiang, Hubei, China, in 1972. He received the bachelor's and master's degrees from the Hubei Institute of Technology and the Ph.D. degree from Chongqing University. He is currently a Professor with the School of Electrical and Electronic Engineering, Hubei University of Technology. He is involved in the online monitoring and fault diagnosis of high voltage electrical insulation equipment, alternative gases of SF_6, the decomposition mechanism of insulating gas SF_6, and the new nano-sensor